

Title Page

■Classification:

Major Category: Physical Science

Minor Category: Chemistry

■Title:

Engineering and Understanding Emergent Properties in Oil Droplet Protocell Behaviours using Artificial Intelligence

■Author Affiliation:

Author name

Laurie J. Pointst†

James Ward Taylor†

Jonathan Grizout†

Kevin Donkerst†

Leroy Cronin†

Address

† WestCHEM, School of Chemistry, University of Glasgow, Joseph Black Building, University Avenue, Glasgow G12 8QQ, U.K.

■Corresponding Author:

Name

Prof. Leroy Cronin

Address

School of Chemistry, University of Glasgow, Joseph Black Building, University Avenue, Glasgow G12 8QQ, U.K.

e-mail:

L.Cronin@chem.gla.ac.uk

Phone:

+44 141 3306650

FAX:

+44 141 3304888

Abstract

Protocells are minimal cell-like entities widely used to explore how the first cells might have assembled at the advent of life on Earth, and for their potentially useful functions as materials. This is because protocells are often very simple, with a limited number of components, but can display complex and varied behaviours. How these complex behaviours can be understood and how these chemicals can be orchestrated to come together and yield life-like systems remain key questions. Herein, starting from a large collection of 7767 droplet experiments collected on a closed loop artificial intelligence robot platform, we develop novel analytical methods providing us with insights into the intricate underlying dynamics of our oil droplet protocell system. Machine learning algorithms enabled the identification of connections between the physical properties and behaviours of droplets, as well as the prediction of new formulations likely to exhibit a rare behaviour - droplet swarming. Furthermore, using ^1H NMR spectroscopy and a pH indicator we were able to better understand oil dissolution, chemical change, phase transitions and droplet and aqueous phase flow. Finally, we designed a new robot to explore the oil and aqueous phase composition simultaneously using a genetic algorithm. Droplets thus showed more varied and extreme behaviours hinting at the complexity inherent in such systems. We argue that cheap, customisable automated platforms used in conjugation with advanced algorithms can benefit a wide range of research areas including complex systems, synthetic and materials chemistry.

Significance Statement

Exploring and understanding the emergence of complex behaviours is difficult even in 'simple' chemical systems since the dynamics can rest on a knife edge between stability and instability. Herein, we study the complex dynamics of a 'simple' protocell system, comprising four component oil droplets in an aqueous environment using an automated platform equipped with artificial intelligence. The system autonomously selects and performs oil in water droplet experiments, and then records and classifies the behaviour of the droplets using image recognition. The data acquired is then used to build predictive models of the system. Physical properties such as viscosity, surface tension, and density are related to behaviours, as well as to new droplet behavioural niches, such as collective swarming.

Introduction

There is great interest in oil-in-water droplets both as protocell models and as simple systems that display an astonishingly delicate set of behaviours that rest on a sensitive knife edge between stability and instability.(1) They have been shown to exhibit cell like properties including movement, division and chemotaxis whilst inherently satisfying the need for a protocell to be compartmentalised.(2-5) The understanding of the driving forces influencing these droplets is limited, although Marangoni instabilities, imbalances in surface tension initiated by symmetry breaking, are thought to play a key role.(6) Indeed, along with autocatalytic systems(7-9), chemical gardens(10, 11) and other protocell models,(12, 13) these systems together illustrate how the combination of relatively few components and phase boundaries can lead to complex and 'life-like' outcomes. Chemotaxis(14, 15) movement in response to chemical stimuli such as a pH or salt concentration gradient, has also been observed in simple oil-in-water droplet systems.(3, 4, 16-18) These oil droplet behaviours are thought to be driven by Marangoni instabilities originating from surface tension asymmetry and by the relative solubilities of the oil and aqueous phase components.(6, 19)

The use of automation and image analysis in the exploration of protocell and droplet systems has been shown to be a powerful way to investigate the behaviours observed for a four-component oil-in-water droplet system.(2) This is because these platforms are now easy to design and construct using affordable and open-source hardware and software. For example, bespoke closed-loop systems can be used for the robotic exploration and assisted evolution of physicochemical systems, expanding from the fields of engineering and robotics, and inspired from the realm of biology.(20-24) The variation in droplet behaviours as their composition varied can be vast and unpredictable, despite having only a small number of inputs. For example,(2) when using only four oil inputs droplets could move rapidly, remain stationary, divide into many smaller droplets, deform or display a whole range of behaviours. The issue is that the systems seem so complex that deriving mechanistic and predictive information seems far from reach.

Herein, we first apply classic analytical chemistry techniques and machine learning to try to expand understanding of our oil-in-water droplet system and to develop analytical methods universally applicable to such systems. The droplets are composed of four oils (octanoic acid, diethyl phthalate (DEP), 1-octanol and 1-pentanol) and are placed in a high pH surfactant containing aqueous phase. The utilisation of machine learning for the prediction of the surface tension and viscosity of the oil mixtures enables the correlation of these to droplet behaviours. pH indicators are shown to be a method suitable for visualising the flow of material within and outside the oil droplets whilst ^1H NMR spectroscopy is used to quantify the level of oil dissolution in the aqueous phase. Furthermore, we present a chemorobotic platform developed to allow us to study how the chemical environment of the droplets (i.e. the aqueous phase) influences the droplet's behaviours by adding up to six aqueous phase constituents. Using the platform we screen for interesting droplet behaviours and utilise a genetic algorithm to optimise both the oil and

aqueous phases simultaneously, thus showing that the co-evolution of an entity with its environment allows the discovery of behavioural niches unreachable by independent evolution. Fundamentally, the combination of physicochemical analysis, machine learning and robotically assisted evolution has allowed significant advances to be made in understanding the mechanism behind droplet behaviours and moved us closer to being able to predict them.

Results

Our system comprises oil droplets (composed of octanoic acid, DEP, 1-octanol and 1-pentanol) placed into a surfactant containing aqueous phase by a robotic assistant. The droplet behaviour is recorded, analysed by computer vision and fed back to generate the next experiments via a genetic algorithm, in a closed loop system (Figure 1). Using this system, 7767 experiments were previously undertaken aimed at exploring the behaviours possible in this system and optimising for three – movement, division and vibration. This represented a vast underexplored dataset which we wanted to exploit to try and investigate the mechanisms behind the behaviours observed in our system. Furthermore, we have now expanded the system to allow the simultaneous variation of the aqueous phase.

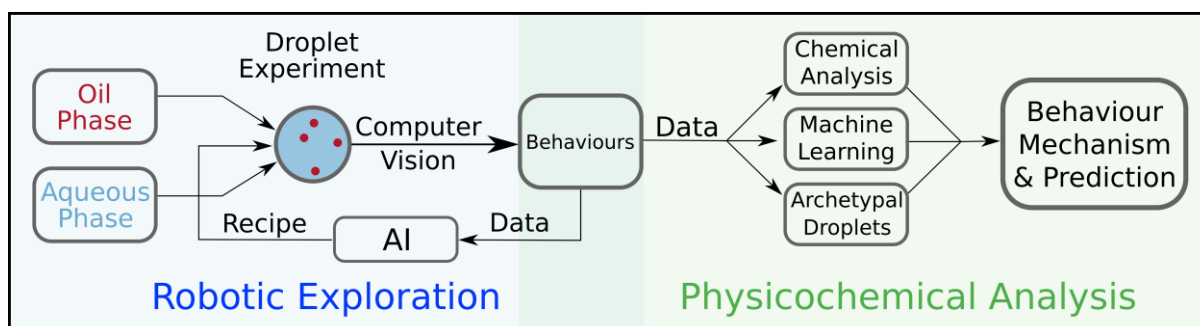


Figure 1 - A summary of the workflow presented herein. During robotic exploration, oil droplets are placed into a surfactant containing aqueous phase by a robotic assistant. The droplet behaviour is recorded, analysed by computer vision and fed back to generate the next experiments via a genetic algorithm, in a closed loop system. The recipes and data generated from this process are then used for physicochemical analysis, where traditional chemical analysis, machine learning and archetypal droplet experiments are used to study the behavioural mechanisms and to predict droplet behaviours.

Chemical Analysis

We hypothesized that the various behavioural effects observed in the previously reported system are due to a trade-off between different oil properties (e.g. density, surface tension and viscosity) and oil dissolution (Figure 2). We targeted our investigations on a select number of archetypal formulations known to exhibit behaviours representative of what is possible in the system. In the subsequent sections we present analysis of the oil density, dynamic viscosity and surface tension, showing how these properties can be related to droplet behaviour. To do this we utilise machine learning techniques – the utility of which is rapidly being demonstrated across the physical sciences.(25-28) Phenolphthalein is used

to investigate phase mixing and material flows whilst ^1H NMR enables quantification of oil dissolution in the aqueous phase.

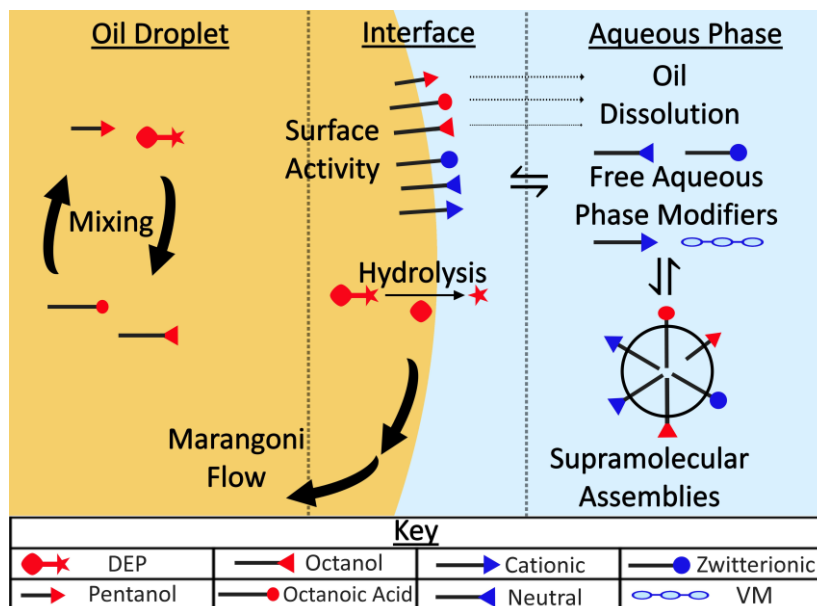


Figure 2 - A summary of the different physical and chemical processes thought to be occurring in our oil-in-water droplet system. VM = viscosity modifier.

A number of oil formulations were prepared and their density, dynamic viscosity and surface tension measured, with the intention of testing for any correlation between these physical properties and droplet behaviour. From this initial dataset, it was clear that for density a simple weighted mean was sufficient for predicting mixed oil formulation densities (see Figure 3). For viscosity, however, an Arrhenius based method yielded unsatisfactory results for dynamic viscosity prediction whilst no appropriate method for surface tension prediction of oil mixtures could be found. As such, machine learning regression was utilised for the prediction of the physical properties of all the formulations previously tested – some 7767 experiments – and mined for trends.

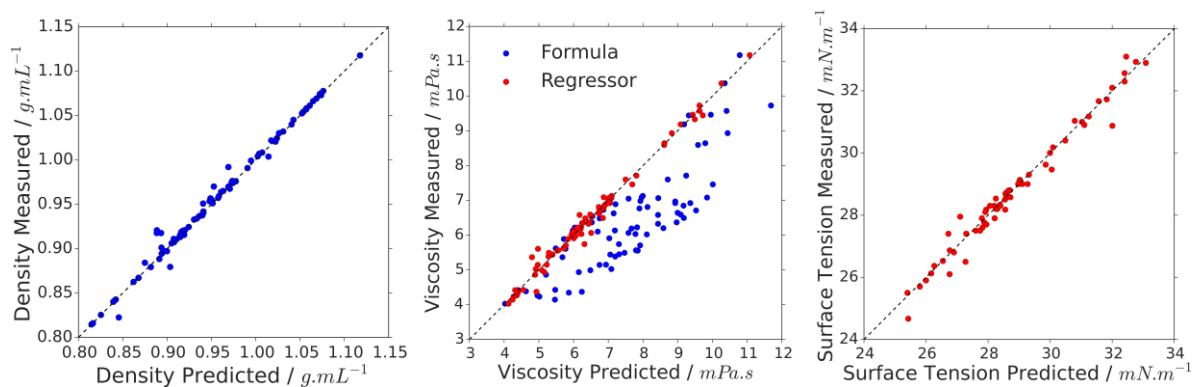


Figure 3 - Plots of the predicted density (left), dynamic viscosity (centre) and surface tension (right) against their measured values. Blue points are predicted using weighted mean (density) and Arrhenius based method (viscosity) whilst red values are predicted using an SVM regressor.

Figure 4 reveals definite correlations between the physical properties of a given oil mixture and how the droplets behave. These plots are presented in full in Supplementary Video 1. For example, oil formulations expressing high levels of division usually have a high density for their surface tension and viscosity and a high surface tension for their viscosity. Similarly, high movement is expressed for formulations with a broad range of intermediate physical properties whilst vibration occurs at the opposite end of the physical property space to division. These trends were confirmed using a machine-learning approach to predict the behavioural trends from oil physical properties, as shown in Supplementary Figure 2. This is significant as it allows us to build a property to behaviour model that fills the gaps between observations.

To test whether we could use physical properties in a predictive manner, we identified two non-overlapping regions in the physical property space where a swarming behaviour (see Automated Experiments section) appeared to be favoured. The physical properties of these formulations were predicted and used to select similar recipes that had not previously been analysed by eye. By repeating these experiments, 20 of the 53 exhibited swarming in both repeats (Supplementary Figure 5), demonstrating that our predicted physical properties could be used to discover more instances of a rare behaviour. Both regions occurred at low viscosity and surface tension, but one at significantly higher density (0.92-0.96 g mL^{-1} vs 0.85-0.88 g mL^{-1}). Prediction of physical properties is therefore a useful tool for both identifying general trends and for identifying new recipes that display a previously observed behaviour.

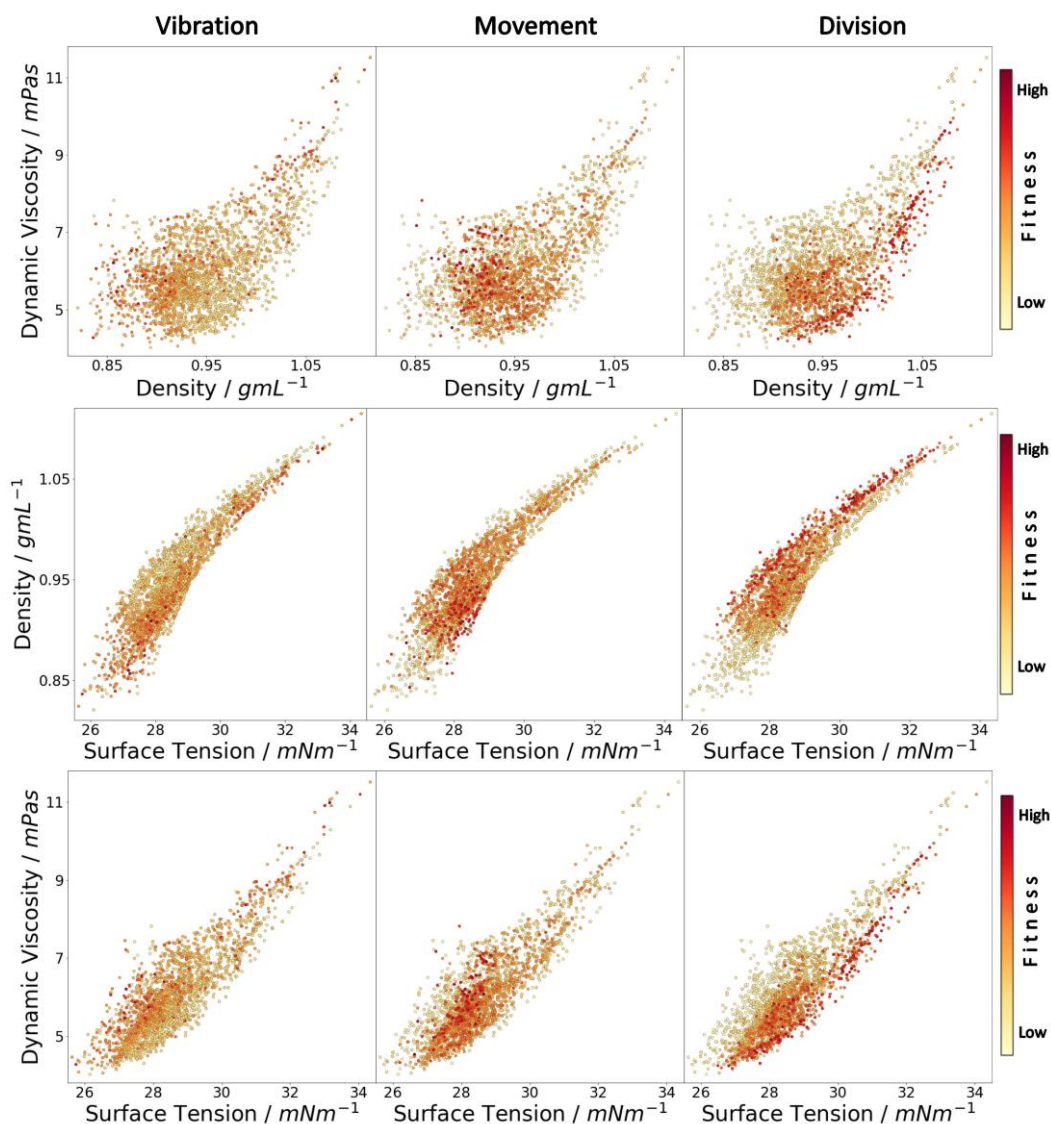


Figure 4 – Impact of dynamic viscosity, density and surface tension on droplet behaviour: movement (left), vibration (centre) and division (right). Each dot is an experiment, the colour is proportional to the intensity of the behaviour.

To investigate phase mixing and material flows, we added a pH indicator - phenolphthalein - to the oil phase. Upon droplet placement the clear, neutral indicator may be deprotonated and turn pink. These experiments confirmed that there is aqueous-oil phase mixing going in both directions – both the oil and aqueous phase end up stained pink, whilst clouds of pink were often seen to diffuse out of the droplets. Furthermore, vastly different effects between the different oils were observed, for example, DEP tends to favour mixing at the boundary and gentler internal mixing whilst pentanol favours rapid internal mixing, as illustrated in Supplementary Video 2. They also show the complexity of the system – the fact that such complex behaviours can be exhibited in such simple systems is remarkable. Supplementary Video 3 shows the Sudan III (red dye) and phenolphthalein (pH indicator) versions of the same four component formulations and illustrates how much more information is accessible using the indicator. Whilst the presence of the indicator will have some effect on the droplet properties, these videos demonstrate that

the effect is minimal. In some cases droplets expel white or pink material and influence the behaviour of nearby droplets, suggesting that matter expelled from the droplets affected the Marangoni forces resulting in chemotaxis. This visualisation of the ‘tethering’ of droplets is both interesting and surprising. The indicator observations were fairly consistent for the same formulation, but different formulations with a high fitness for a particular behaviour did not exhibit identical indicator phenomena.

Hypothesising that oil dissolution could play a role in droplet behaviour, we developed an experimental procedure to quantify the amount of each oil dissolved in the aqueous phase. Interestingly, ethanol was present in the aqueous phase, due to the hydrolysis of DEP, showing that, even in this simple system, both physical and chemical processes take place. Initially, we focused on droplets containing either a single oil or a 1:1 (v/v) mixture of two oils.

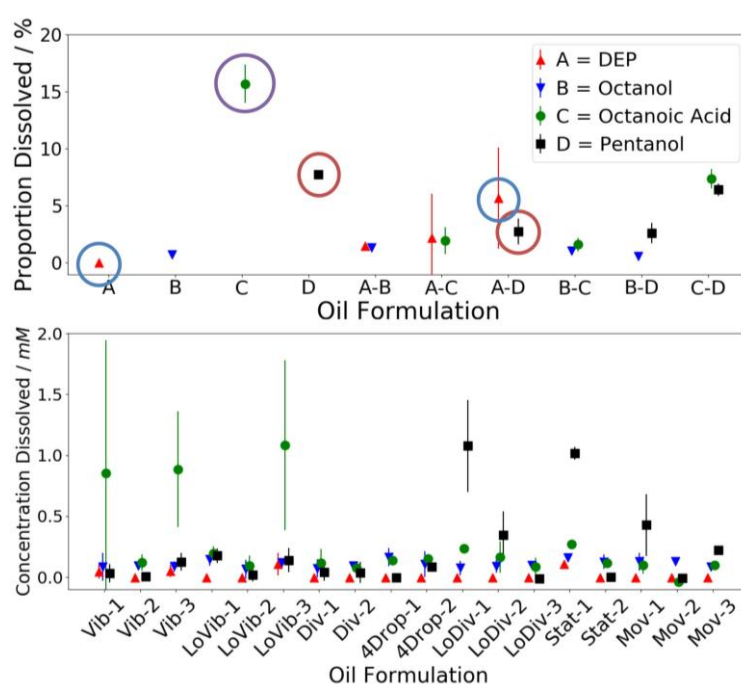


Figure 5 – Plots showing the concentration of oil dissolved in the aqueous phase for various formulations 1 minute after $4 \times 4 \mu\text{L}$ droplets are placed in 3.5 mL aqueous phase. Top panel: The proportion of the oil present dissolved for droplets composed of a single oil or 1:1 (v/v) mixture of 2 oils. i.e. point A-B corresponds to the oil dissolution levels when a 1:1 (v/v) mixture of DEP and octanol is used as the droplet formulation. Lower panel: The concentration oil dissolved for full 4 oil formulations, categorised by the high or low fitnesses they show for certain behaviours. Key: Vib, LoVib – High or low vibration fitness. Div, LoDiv - High or low division fitness. 4Drops – A division fitness of 4 – i.e. 4 droplets present after 1 minute. Mov, Stat – High or low movement fitness. Error bars show SD.

As can be seen from Figure 5, there are significant variations in the levels of oil dissolution depending on the oil formulation present. When placed alone, octanoic acid and pentanol dissolve to significant levels (red and purple circles), whilst DEP is not seen to dissolve at all (blue circle), as expected given the oils’ aqueous solubilities. The trend for the binary mixtures are not, however, as predictable. Octanoic acid and pentanol promote the dissolution of the other oils, whilst simultaneously their own

dissolution is lower. Octanoic acid is seen to dissolve at low levels when mixed with DEP, octanol or even pentanol. These observations could either be due to molecular scale interactions or due to droplet behaviour. On observing how each of the binary oil droplet behaves, however, there does not appear to be a direct link between oil dissolution and droplet behaviour in these cases. For those cases with large error bars, it is thought this is due to spatiotemporal variations in the oil concentration within each experiment.

For full formulations the levels of oil dissolution are similar, but for a few outliers. These formulations represent a vast range of droplet behaviours, thus implying that the level of oil dissolution does not play a key role in defining droplet behaviour. There are some exceptions, however. For example, three formulations show significantly higher levels of octanoic acid dissolution than the rest of the formulations. On viewing the phenolphthalein indicator videos of these formulations, these are also the only formulations that show a ‘tethering’ interaction between droplets, thus implying there is a link between octanoic acid dissolution and this interaction, potentially with octanoic acid aqueous phase supramolecular assemblies playing a key role. The level of pentanol dissolution is also seen to vary significantly, although in almost all cases this is just a reflection of the changing level of pentanol in the formulation, as pentanol has a relatively high water solubility. It is very interesting to know that oil dissolution does not play a key role in the quantified droplet behaviours but can be linked to other observed effects.

Automated Experiments

To investigate how the chemical environment of the droplets (i.e. the aqueous phase) influences their behaviour we wished to enable the simultaneous variation and optimisation of both the aqueous and oil phases. A robotic platform was designed to automatically undertake droplet experiments with variable aqueous and oil phases, with droplet analysis via video recording (Supplementary Figure 7, Supplementary Video 4). Six aqueous phase modifiers were chosen for use on the automated platform: the cationic surfactants TTAB and CTAB; the non-ionic surfactants Brij O10 and Triton X-100; the zwitterionic surfactant DDMAB and poly(ethylene glycol) ($M_n = 400$). These were chosen due to their varied chemical structures, properties, effects on droplets and compatibility. To identify the droplet behaviours possible in this new system, 393 random recipes were tested. Movement and division, as previously observed with the single aqueous phase system, were again the most prevalent droplet behaviours. Remarkably, several new behaviours were identified: swarming, fusion, pulsing and sorting (see Supplementary Video 5).

‘Swarming’ was observed when the droplets divided into a large number of small droplets on placement, maintaining a close proximity to each other whilst appearing to move in concert, as illustrated in Figure 6. Interestingly, if a larger droplet approached the swarm of smaller droplets, the direction and

shape of the whole swarm changed in response to repulsive interactions. From our analysis work we have some understanding of the driving forces behind this swarming behaviour. Initially, a large number of droplets must be present – hence the formulation must be unstable leading to rapid division. Following this, small droplets either move collectively, apparently driven by bulk surface tension variations ‘carrying’ the droplets together; or the smaller droplets are ‘herded’ by larger droplets, whose more definite movements through the swarm cause the swarm to shift around the larger droplet. Often, there is a period of rapid division at the beginning of the experiment followed by a period of swarming and then the repeated fusion of the small droplets.

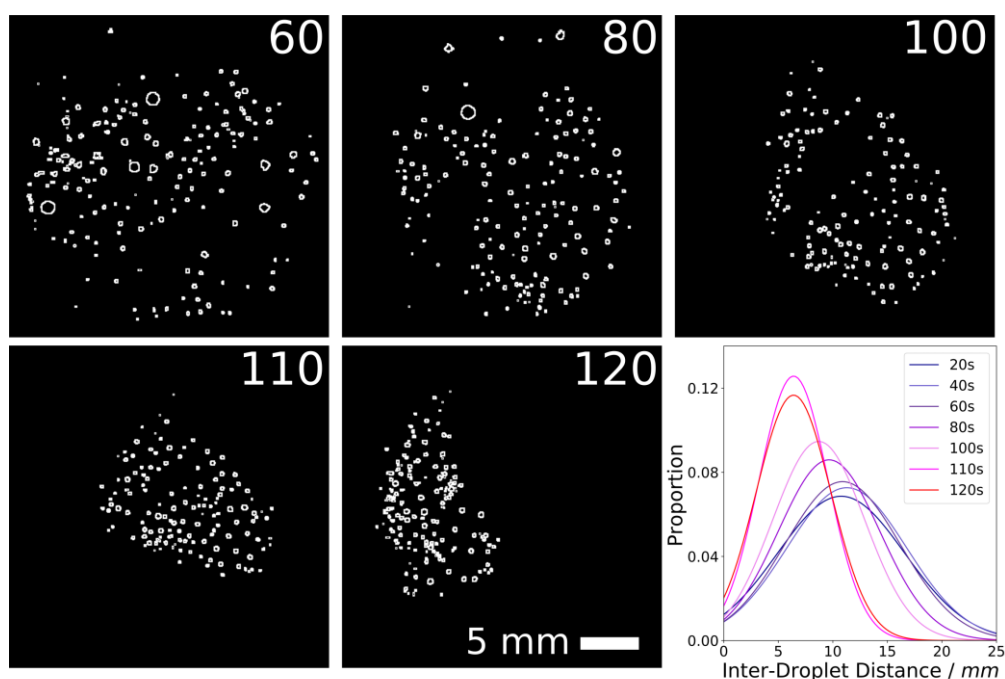


Figure 6 – Video snapshots of a swarming formulation, converted into black and white outlines using ImageJ. Numbers in the corners correspond to the experiment time in seconds since the experiment started. Initially there are relatively few droplets, fairly evenly spaced (0-60s). These then divide and swarm, to give more droplets closer together. At around 100-105 s, the rapid dissolution of a droplet stuck to the edge of the dish (not shown), leads to a much tighter knit swarm, with an average inter-droplet distance of only around 6.4 mm. The variation in inter-droplet distance is also seen to decrease. Images processed using ImageJ.(29)

Droplet ‘fusion’ had previously been observed in the TTAB only system, but it was very rare owing to the stabilising boundary formed by the cationic surfactant. It would, however, be a desirable behaviour for oil droplets to exhibit, especially if it can be controlled, due to the possibility of controlling a chemical reaction between two components dissolved in two separate droplets. Electrostatic repulsion plays a role in the prevention of fusion, in addition to surfactant gradients induced by the decrease of distance between droplets resulting in Marangoni forces against the direction of movement.(30) These forces can be reduced by ion-pairing between oppositely charged ions (e.g. quaternary ammonium surfactant and octanoate). Clusters of many smaller droplets provide greater surface area for the deprotonation of

octanoic acid, which combined with cationic surfactants in the aqueous phase forms a catanionic system. Indeed, fusion is far more commonly observed for smaller droplets and division for larger droplets, implying there may be an intermediate optimal radius in many cases. As surfactant concentrations vary, fluctuations in interfacial tension mean that division could be favoured in one location in the dish and fusion in another.(31) Some droplet formulations give droplets which may fuse if they happen by chance to collide with each other, i.e. they have no significant repulsive or attractive forces, whilst others exhibit attraction to each other and experience a change of trajectory before fusion. 'Pulsing' droplets exhibit constant, rapid changes in diameter as the droplets shrink and grow periodically. This is in contrast to vibration, which involves rapid changes in a droplet's direction of movement. When droplets were attracted to the walls of the petri dish they sometimes also exhibit movement around the edge of the dish, division or fusion. This also often resulted in droplet 'sorting', in which the droplets spread themselves evenly around the circumference of the dish due to repulsive interactions between the droplets.

Having identified the behaviours possible in this system, a genetic algorithm optimization was then carried out for movement using all ten components. CTAB and Brij-O10 were quickly optimized out almost entirely (Supplementary Figure 6), thus only the remaining four aqueous phases were subsequently used. It is very interesting to note that TTAB and CTAB, which differ only by two CH₂ groups to the surfactant tail, have such different effects on droplet behaviour. The results of a genetic algorithm optimization for movement (average speed of the droplets) with these eight parameters are shown in Figure 7a. With these eight inputs there are 9.2×10^{15} possible recipes, a space unfeasible to search exhaustively. The genetic algorithm was run for 30 generations, with 10 new recipes each generation, taking approximately 80 hours for a complete optimization. The optimization was repeated in triplicate from random starting recipes, and compared with the maximum fitness values observed in the oil only experiments. The final median fitness value of each individual GA run surpassed 5.37 mm s^{-1} , whilst the maximum fitness value achieved was 9.59 mm s^{-1} . This compares to the oil only optimisations which achieved a maximum droplet speed of 7.17 mm s^{-1} and a median of up to 4.78 mm s^{-1} . The large increase in median fitness from less than 1.0 up to $5.37 - 6.93 \text{ mm s}^{-1}$ showed that the environment in which the droplets are placed has a considerable influence on their movement, and that the higher number of parameters used in the optimization enabled even higher fitnesses to be observed. Supplementary Figure 9 shows the evolution of the composition of both the aqueous and oil phases during the evolutionary experiments. Overall, the compositional trajectories and final values differ significantly between runs while the upward trend in

fitness is conserved, illustrating the complexity of the system and why it is beneficial to optimise the aqueous and oil phases together. Interestingly, as Supplementary Figure 10 shows, the physical properties of the oil phase are fairly consistent throughout the runs, despite this compositional variation.

To investigate whether such high fitnesses could be observed by first optimising the oil phase and then the aqueous phase, instead of optimising them simultaneously, evolution experiments were carried out with a predefined high fitness oil formulation optimised in the TTAB only aqueous phase (Supplementary Figure 11). The recipe chosen had a high, reproducible movement fitness value of 5.96 mm s^{-1} . The oil droplet fitness again increased throughout the optimisation, but only by $1\text{-}2 \text{ mm s}^{-1}$, in contrast to approximately 6.0 mm s^{-1} in the case of the 8 parameter evolution experiment. Only one of the three runs surpassed the fitness previously observed with 100 % TTAB aqueous phase suggesting that 100 % TTAB was close to the optimal aqueous phase for this oil formulation, even though much higher fitnesses are attainable with different oil-aqueous formulations. Supplementary Video 6 compares the fastest moving droplets from each of these evolution experiments.

The evolutionary trajectories were compared between the oil only, aqueous only and combined optimizations (Figure 7a). The oil only optimization began from the highest fitness value compared to the others, closely followed by the aqueous only optimization. In contrast, the combined optimization of aqueous and oil phases began at a fitness value of below 1.0 mm s^{-1} , far lower than the other runs, which both began with one phase closer to optimal. With the composition of both phases completely randomized for all individuals in the first generation, the low median fitness demonstrates that the 8 parameter space is vast and contains many more poor formulations for a given fitness criterion than good ones. The increase in fitness over successive generations is rapid, and leads to a much higher final fitness than for either of the separate optimizations. This demonstrates the complexity of the formulation space - an oil phase which is optimal for one aqueous phase may give poor results in another aqueous phase, and vice versa, yet when both phases are optimized together, the full range of effects of each component on the others is taken into account, and therefore a greater space is available to the algorithm for exploration.

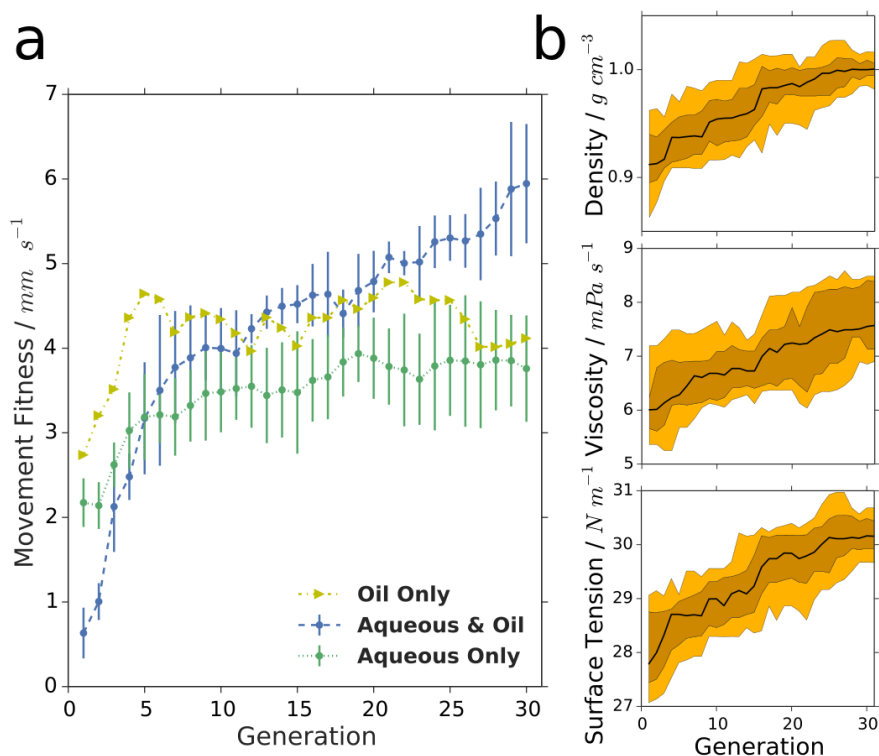


Figure 7 – a) - Comparison of median fitness values for each generation between the oil only, aqueous only, and simultaneous aqueous and oil optimizations. Error bars show SD. b) Change in physical properties of the oil mixture vs generation for the aqueous & oil phase optimization (run 1). The black line corresponds to the median for each generation, the dark yellow area shows the distribution between the 75th and 25th percentile, and the pale yellow area shows the distribution between the 90th and the 10th percentile.

Discussion

Three novel analytical methods have been developed for the analysis of oil in water droplet systems – formulation physical property prediction based on machine learning methods, quantification of oil dissolution using ¹H NMR spectroscopy and the use of a pH indicator to visualise phase mixing and flows. Through density, viscosity and surface tension prediction, correlations have been identified between physical properties and droplet behaviours. This also allowed the prediction of recipes exhibiting a rare droplet behaviour – swarming. ¹H NMR spectroscopy has shown that, despite a massive range of droplet behaviours, the levels of oil dissolution are generally constant for all recipes. This implies that oil dissolution is not the key factor defining droplet behaviour. It is our intention, however, to further develop this method via sampling at different times and locations – maybe dissolution kinetics varies in a way not captured by our end point method. Finally, the use of a pH indicator has opened a window into the droplet and aqueous phase dynamics. Specifically, long range ‘tethering’ interactions have been identified between droplets, which seems to be linked to octanoic acid dissolution in the aqueous phase. Notably, the three analytical methods developed complement each other; one is a measure of bulk properties, one is a measure of the state of the system and the other allows visualisation of spatiotemporal variations

within the system. Particularly, the NMR and indicator studies fill a gap in the physical property prediction in that they study dynamic processes occurring, not just bulk properties.

By expanding our droplet system to include the aqueous phase, using different surfactant types and modifiers, new droplet behaviours were observed. The increased speed of the droplets accessible when both phases (eight parameters) were optimized together (over oil or aqueous phase in isolation) shed light on the complexity and intertwined physicochemical properties of our droplet system. With eight parameters a complete exploration of all possible combinations would take 2.1×10^{11} years with our platform, making artificial intelligence an indispensable tool. Evolution *in materio*, using artificial intelligence in combination with a liquid handling robot for autonomous exploration of chemical spaces is rapidly proving its utility for tackling wider chemical problems. Over and above work utilising oil-in-water droplets, we believe that cheap, robust and customisable automated platforms, in conjugation with advanced computer science methods, represent a hugely underdeveloped opportunity for chemists to apply to a wide range of research areas including complex systems, chemical synthesis and materials chemistry. Of particular interest are recent developments on novelty seeking and curiosity driven algorithms that opens the way to the genuine autonomous exploration of what can be done with a new system rather than a more directed optimization of a specific property.(32, 33) In the future, we hope to apply these methods to other systems, to further show the benefits possible via the interaction of these fields.

Materials and Methods

Detailed materials and methods are given in the supporting information. The robotic platform used within this work is based upon that previously reported by this group, modified to allow the use of multiple aqueous phase constituents.(2) Due to the need for maximum consistency throughout experiments, standard operating procedures were developed for oil and aqueous phase preparation which are shown in the supporting information. Aqueous phases were prepared with a 20 mM concentration of the given modifier at a pH of c. 13 whilst the oils were dyed with 0.25 mg mL^{-1} Sudan III dye. For each droplet experiment, $4 \times 4 \mu\text{L}$ droplets were placed into 3.5 mL of mixed aqueous phase and a 1 minute video recorded for analysis via computer vision.

Experiments based on Physical Property Prediction

For physical property prediction, the viscosity and density of 81 formulations were measured, whilst the surface tension of 69 oil formulations were measured using the Du Noüy ring method. A weighted mean was then deemed sufficient for density prediction, whilst a SVM regressor using a 'RBF' kernel was used for viscosity and surface tension prediction. For the discovery of new swarming formulations the density, viscosity and surface tension of 5 known swarming formulations were calculated. The range of physical properties from each group of swarming formulations were used to find formulations within

them that could be tested and analysed for swarming behaviours. 53 formulations were tested in duplicate, of which 20 exhibited swarming in both repeats, with a further 10 showing swarming in one of the two repeats.

Random Matrix Screen

A proximity-limited random search was carried out in 10 dimensions (6 aqueous, 4 oils), using a threshold factor to ensure formulations generated were sufficiently different, 393 random formulations were tested.

Genetic Algorithm Explorations

A genetic algorithm was used with a genome length equal to the number of components for the mixture. 24 random combinations were tested to form generation 1, then roulette wheel selection was used to select individuals carried over to undergo crossover and random mutation - forming the next generation of 10 individuals. The experiment was continued for 30 generations. An individual's fitness was quantified using the previously published methodology.(2)

Author Contributions

L.C., L.J.P. and J.W.T. conceived the idea. L.J.P. undertook chemical analysis work with J.G. providing assistance and supervision. L.J.P, J.W.T. and K.D. designed and constructed the robotic hardware and software and undertook the automated experiments and analysis. L.J.P., J.W.T., J.G. and L.C. co-wrote the manuscript and J.G. lead the team that helped do this work.

Acknowledgements

ACKNOWLEDGE FUNDING. We thank Dr. Salah Sharabi for assistance with hardware and electronics, Dr. Sergey Zalesskiy for assistance with ¹H NMR spectroscopy experiments, Kliment Yanev for providing the base platform and Dr Juan Manuel Parrilla Gutierrez. We gratefully acknowledge financial support from the EPSRC for funding (Grant Nos EP/H024107/1, EP/I033459/1, EP/J00135X/1, EP/J015156/1, EP/K021966/1, EP/K023004/1, EP/K038885/1, EP/L015668/1, EP/L023652/1), BBSRC (Grant No. BB/M011267/1), the EC (projects 610730 EVOPROG, 611640 EVOBLISS), LC thanks the Royal Society / Wolfson Foundation for a Merit Award and the ERC for an Advanced Grant (ERC-ADG, 670467 SMART-POM).

References

1. Lach S, Yoon SM, Grzybowski BA (2016) Tactic, reactive, and functional droplets outside of equilibrium. *Chem Soc Rev* 45:4766–4796.

2. Gutierrez JMP, Hinkley T, Taylor JW, Yanev K, Cronin L (2014) Evolution of oil droplets in a chemorobotic platform. *Nat Commun* 5:5571.
3. Hanczyc MM, Toyota T, Ikegami T, Packard N (2007) Fatty acid chemistry at the oil - water interface: self-propelled oil droplets. *J Am Chem Soc* 129(30):9386–9391.
4. Lagzi I, Soh S, Wesson PJ, Browne KP, Grzybowski BA (2010) Maze solving by chemotactic droplets. *J Am Chem Soc* 132:1198–1199.
5. Dzieciol AJ, Mann S (2012) Designs for life: protocell models in the laboratory. *Chem Soc Rev* 41(1):79–85.
6. Schmitt M, Stark H (2016) Marangoni flow at droplet interfaces: Three-dimensional solution and applications. *Phys Fluids* 28(1):12106.
7. Bissette AJ, Odell B, Fletcher SP (2014) Physical autocatalysis driven by a bond-forming thiol-ene reaction. *Nat Commun* 5:4607.
8. Ortega-Arroyo J, Bissette AJ, Kukura P, Fletcher SP (2016) Visualization of the spontaneous emergence of a complex, dynamic, and autocatalytic system. *Proc Natl Acad Sci* 113(40):11122–11126.
9. Bottero I, Huck J, Kosikova T, Philp D (2016) A synthetic replicator drives a propagating reaction–diffusion front. *J Am Chem Soc* 138(21):6723–6726.
10. Haudin F, Cartwright JHE, Brau F, De Wit A (2014) Spiral precipitation patterns in confined chemical gardens. *Proc Natl Acad Sci* 111(49):17363–17367.
11. Barge LM, et al. (2015) From chemical gardens to chemobionics. *Chem Rev* 115(16):8652–8703.
12. Qiao Y, Li M, Booth R, Mann S (2017) Predatory behaviour in synthetic protocell communities. *Nat Chem* 9:110–119.
13. Engelhart AE, Adamala KP, Szostak JW (2016) A simple physical mechanism enables homeostasis in primitive cells. *Nat Chem* 8:448–453.
14. Adler J, Tso W-W (1974) “Decision”-Making in bacteria: chemotactic response of escherichia coli to conflicting stimuli. *Science* 184(4143):1292–1294.
15. Van Haastert PJM, Devreotes PN (2004) Chemotaxis: signalling the way forward. *Nat Rev Mol Cell Biol* 5(8):626–634.
16. Toyota T, Maru N, Hanczyc MM, Ikegami T, Sugawara T (2009) Self-propelled oil droplets consuming “fuel” surfactant. *J Am Chem Soc* 131(14):5012–3.
17. Miura S, et al. (2014) pH-induced motion control of self-propelled oil droplets using a hydrolyzable gemini cationic surfactant. *Langmuir* 30(27):7977–7985.

18. Čejková J, Novák M, Štěpánek F, Hanczyc MM (2014) Dynamics of chemotactic droplets in salt concentration gradients. *Langmuir* 30(40):11937–11944.
19. Scriven LE, Sternling C V. (1960) The Marangoni Effects. *Nature* 187(4733):186–188.
20. Eiben AE, Kernbach S, Haasdijk E (2012) Embodied artificial evolution: Artificial evolutionary systems in the 21st Century. *Evol Intell* 5(4):261–272.
21. Harding SL, Miller JF, Rietman EA (2008) Evolution in materio: Exploiting the physics of materials for computation. *Int J Unconv Comput* 4:155–194.
22. Hornby GS, Lohn JD, Linden DS (2011) Computer-automated evolution of an X-band antenna for NASA's Space Technology 5 mission. *Evol Comput* 19(1):1–23.
23. Eiben AE, Smith J (2015) From evolutionary computation to the evolution of things. *Nature* 521(7553):476–482.
24. Gould SJ (1982) Darwinism and the expansion of evolutionary theory. *Science* 216(4544):380–387.
25. Jordan MI, Mitchell TM (2015) Machine learning: Trends, perspectives, and prospects. *Science* 349(6245):255–260.
26. Raccuglia P, Elbert KC, Adler PDF, Falk C, Wenny MB, Mollo A, Zeller M, Friedler SA, Schrier J, Norquist AJ. (2016) Machine-learning-assisted materials discovery using failed experiments. *Nature* 533(7601):73–76.
27. Carleo G, Troyer M (2017) Solving the quantum many-body problem with artificial neural networks. *Science* 355(6325):602–606.
28. Smith JS, Isayev O, Roitberg AE (2017) ANI-1: An extensible neural network potential with DFT accuracy at force field computational cost. *Chem Sci* 8:3192–3203.
29. Schneider C A, Rasband WS, Eliceiri KW (2012) NIH Image to ImageJ: 25 years of image analysis. *Nat Methods* 9(7):671–675.
30. Baret J-C (2012) Surfactants in droplet-based microfluidics. *Lab Chip* 12(3):422–33.
31. Caschera F, Rasmussen S, Hanczyc MM (2013) An Oil Droplet Division – Fusion Cycle. *Chempluschem* 78(1):52–54.
32. Lehman J, Stanley KO (2008) Exploiting open-endedness to solve problems through the search for novelty. *Artif Life XI (Alife Xi)*:329–336.
33. Oudeyer PY, Kaplan F, Hafner V V. (2007) Intrinsic motivation systems for autonomous mental development. *IEEE Trans Evol Comput* 11(2):265–286.

Further Supplementary References

1. Gutierrez, J. M. P., Hinkley, T., Taylor, J. W. & Yanev, K. Hardware and Software manual for Evolution of Oil Droplets in a Chemorobotic Platform. *Arxiv* 1–42 (2014).
2. Khalil, M. I., Al-Yami, R. A. H. & Al-Khabbas, M. H. Introducing mole fraction in the density calculations of liquid-liquid solutions. *Int. J. Phys. Sci.* 8, 27–30 (2013).
3. Zhmud, B. Viscosity Blending Equations. *Lube-Tech* 121, 1–4 (2014).
4. *CRC Handbook of Chemistry and Physics*. (CRC Press, 2005).
5. Sangster, J. Octanol-Water Partition Coefficients of Simple Organic Compounds. *Journal of Physical and Chemical Reference Data* 18, 1111–1229 (1989).